Hindawi
Geofluids
Volume 2022, Article ID 5201061, 13 pages
https://doi.org/10.1155/2022/5201061

Research Article

An Experimental Study on Mechanical Properties and Fracture Characteristics of Saturated Concrete under Coupling Effect of Low Temperature and Dynamic Load

Mengxiang Wang,[1,2] **Qi Zong**,[1] **and Haibo Wang**[1]

[1]*School of Civil Engineering and Architecture, Anhui University of Science and Technology, Huainan, 232001 Anhui, China*
[2]*Fujian Provincial Colleges and University Engineering Research Canter of Engineering Quality Testing and Safety Assessment, Longyan 364000, China*

Correspondence should be addressed to Mengxiang Wang; mxwang@aust.edu.cn

Received 21 July 2022; Revised 17 August 2022; Accepted 22 August 2022; Published 20 September 2022

Academic Editor: Yiding Bao

Concrete is widely used in bridge foundation, water supply, and drainage engineering. On the one hand, the saturated concrete is always in the saturated state. In the cold winter, northeast China and the alpine region suffer from freezing disaster. On the other hand, it has to continue to bear the dynamic load action of vehicles and running water, which makes the stress state of saturated concrete more complicated under the coupling action of low temperature and dynamic load. In order to study the mechanical properties and fracture characteristics of saturated concrete under the coupling effect of low temperature and dynamic load, the impact compression tests of concrete under normal temperature 20°C, -5°C, -10°C, and -15°C were carried out with a diameter of 74 mm split Hopkinson pressure bar (SHPB). The stress-strain characteristics, energy dissipation, and failure modes of specimens under different low temperatures were studied. From a detailed point of view, the failure mechanism of low-temperature water-saturated concrete is expounded. The results show that under the same dynamic load, the dynamic stress-strain curve of saturated concrete changes obviously with the change of low temperature. The dynamic compressive strength of the natural specimen at room temperature is high while that of the water-saturated specimen is low, and the dynamic compressive strength is opposite at low temperature. At the same temperature, the energy time-history curves of concrete in the saturated state are different from those in the natural state, mainly in the plastic section. The energy time-history curves of saturated concrete are different at different temperatures, and the energy dissipation rate of saturated concrete increases linearly with the decrease of temperature. Under the experimental conditions, the dynamic strength of saturated concrete increases linearly with the decrease of temperature, and the peak strain of saturated concrete decreases linearly with the increase of temperature. With the decrease of temperature, the fragmentation of saturated concrete under the impact of the same air pressure gradually increases, and the integrity of the specimen gradually improves. Low temperature can improve the impact resistance of saturated concrete, which is consistent with the failure law of natural state concrete. The water-saturated low-temperature state of the concrete void is filled with ice crystal particles; for low-temperature water-saturated concrete in the impact of the dynamic load, the microstructure is affected by the ice crystal structure which is not easy to change; the specimen along the axial force direction microdefect development produces a crack, the crack along the parallel to the pressure direction of cracking, through the two ends of the specimen, and finally produces axial splitting tensile damage. The research results have important theoretical significance for the safety design of low temperature saturated concrete structures.

1. Introduction

Concrete is a typical nonuniform material, widely used in the construction field, bridge foundation, water supply, and drainage engineering; concrete mechanical properties are greatly affected by temperature and humidity. During the construction of Qinghai-Tibet railway, the influence of low temperature environment on the mechanical properties of

concrete cannot be ignored [1–6]. The Nazixia Dam is located in a cold climate, and its concrete slabs are required to be stable at low temperatures [7]. In bridge foundation, water supply and drainage project, immersed concrete faces with frost heaving dangerous under low temperature state, while the structure should continue to bear the dynamic load of vehicles, running water, and so on. Therefore, it is of theoretical and engineering significance to study the mechanical properties and fracture characteristics of saturated concrete under the coupling action of low temperature and dynamic load.

Wang et al. carried out tests on the compressive strength of concrete cubes at -60°C~20°C, and the results showed that the compressive strength of concrete cubes increased linearly with the decrease of temperature within the test range [8]. Zhang e al. tested the compressive strength of concrete under -165°C~0°C and found that the growth was obvious between -40°C and -80°C, while the growth was slow after -120°C [9]. Dahmani et al. found that the properties of concrete at low temperatures are determined by porosity, and the strength of concrete decreases when subjected to freeze-thaw cycles [10]. Domestic scholars also tested the low temperature compressive strength of concrete mixed with different additives (such as rubber, polypropylene fiber, and asphalt) [11–13]. Fang et al. carried out bending-tension tests on ultrahigh performance concrete with discrete short fine steel fibers at -20°C and 20°C. It was found that with the decrease of temperature, the bond between steel fibers and concrete became stronger, the slip between them decreased, and the ductility became smaller [14].

The research on concrete performance at low temperature is mainly limited to static performance and freeze-thaw cycle. There are abundant research achievements on concrete impact test [15–18]. Zhu et al. cured basalt fiber concrete at -30°C and carried out a drop hammer test on the specimens at room temperature. It was found that basalt fiber could improve the impact resistance of concrete at low temperature, and there was a linear relationship between the fiber content and the impact resistance [19]. Huang and Xiao used a 155 mm large-diameter SHPB device to conduct impact compression tests on φ150 mm × 300 mm lightweight high-strength concrete. The failure of concrete specimens is mainly brittle failure. With the increase of impact velocity, the failure degree of specimens will gradually become higher [20]. Yan et al. conducted dynamic compression experiments on concrete with different initial damage degrees and found that the dynamic compressive strength of concrete decreased gradually with the increase of initial damage degrees. When the injury degree is less than 20%, the influence is more significant than 40% [21]. Many experts have also done a lot of research on water saturated concrete [22–24]. Sun et al. conducted acoustic emission test on rock, concrete, and rock concrete as one medium under uniaxial load under dry and saturated conditions and found that the peak value of impact number of saturated specimens was slightly behind that of stress [25]. Wang et al. on natural drying condition studied the water quality change of geological polymer concrete, ultrasonic wave velocity, compressive strength, flexural strength, and splitting strength and analyzed the saturated state of geological polymer (GC) basic physical and mechanical properties of concrete; the influence of saturated state of the GC static mechanics performance has obvious negative impact. Its compressive strength, flexural strength, and splitting strength are lower than those of dry condition [26].

In order to study the mechanical properties and fracture characteristics of saturated concrete under the coupling effect of low temperature and dynamic load, low temperature and saturated concrete were taken as the research object. Impact compression tests of concrete under normal temperature (-5°C, -10°C and -15°C), saturated water, and natural state were carried out by using a diameter of 74 mm split Hopkinson pressure bar (SHPB). The dynamic stress-strain characteristics and failure modes of saturated concrete in different low temperature states were studied, and the dynamic strength, peak strain, absorption energy, and fracture characteristics of specimens were analyzed with low temperature. Compared with natural concrete, the research results have important theoretical significance for the safety design of low temperature saturated concrete structures.

2. Test Design

2.1. Specimen Making and Scheme. Ordinary Portland cement was chosen to cast C40 concrete in the test. The cement is P·O 42.5 ordinary Portland cement produced by Huainan Bagongshan Cement Factory. Gravel for artificial gravel has a nominal particle size of 5~15 mm (continuous grading). Sand is medium fine sand, and particle grade is good, with over 1 mm sieve. Use ordinary tap water. The water-cement ratio of concrete is 0.46, and the mixing ratio C : W : S : G = 1 : 0.46 : 1.48 : 2.20. Concrete was poured with a rectangular template and vibrated with a shaking table. According to the GB/50081-2002 standard, concrete curing is done at temperature of 20 ± 2°C, and relative humidity of >95%. After standard curing for 28 days, the cylinder was taken out, cut, and polished by ZS-100 vertical drilling core machine, and a cylinder specimen of φ 74 mm × 37 mm was obtained, as shown in Figure 1.

In this experiment, two kinds of concrete in saturated and natural state were adopted, and low water-saturated concrete was taken as the main object of study. After 28 days of maintenance, the specimen is treated with water, and in order to ensure that the specimen is in a full state, it is soaked under negative pressure for 72 hours. The freeze-thaw box (as shown in Figure 2) was used to deal with the temperature of the two kinds of concrete at room temperature (-5°C, -10°C, and -15°C). Due to the large discreteness of dynamic experiment, in order to ensure the repeatability of experimental results, five concrete test blocks were selected under the same curing condition during the impact compression test of the sample. Because concrete is thermal inert material, in order to ensure that the temperature of the specimen does not change too much in the test process, a simple insulation box is made, together with the sample into the low-temperature curing box. The test block is then placed into a sealed bag, then put into salt water, and frozen;

Figure 1: Partial sample.

Figure 2: Freeze-thaw box.

the test block is put into the refrigerator; the internal temperature stabilization of the refrigerator requires a process; when the specimen reaches the set temperature, it needs to be stable for 24 hours, so the freezing time is set to 48 hours. During the experiment, it was taken out together with the foam box, and the impact test was carried out quickly to reduce the heat loss inside the concrete specimen and to ensure that the temperature was kept in the effective range during the experiment as far as possible. Before the experiment, the temperature in the simple foam box was measured to meet the requirements of the test temperature.

2.2. Test Device and Test Method. The 74 mm diameter variable section SHPB test device of Anhui University of Science and Technology was used in the impact test, as shown in Figure 3. The length of the impact bar was 0.60 m, and the lengths of the incident bar and transmission bar were 2.40 m and 1.20 m, respectively. The impact bar, incident bar, transmission bar, and absorption bar are all alloy steel with a density of 7.8 g/cm^3, elastic modulus of 210 GPa, and p-wave velocity of 5190 m/s. The type of resistance strain gauge used to collect voltage signals on the incident bar and transmission bar is BX120-2AA, and the strain gauge grid length is 2 mm, which can meet the requirements of dynamic measurement accuracy. CS-1D dynamic strain gauge and TST 3406 dynamic test analyzer were used for data signal acquisition.

Based on one-dimensional stress wave propagation theory, a two-wave method is used to calculate the stress, strain, and strain rate of specimen under impact [27].

$$\begin{cases} \dot{\varepsilon}(t) = \dfrac{2C_0}{l_s}\varepsilon_r(t), \\ \varepsilon(t) = \dfrac{2C_0}{l_s}\displaystyle\int_0^t \varepsilon_r(t)dt, \\ \sigma(t) = \dfrac{A_0E_0}{2A_S}\varepsilon_t(t). \end{cases} \tag{1}$$

The energy carried by incident, reflected, and transmitted waves can be expressed by the following formula [27]:

$$\begin{cases} W_i(t) = AEC_0\displaystyle\int_0^t \varepsilon_i{}^2(t)dt, \\ W_r(t) = AEC_0\displaystyle\int_0^t \varepsilon_r{}^2(t)dt, \\ W_t(t) = AEC_0\displaystyle\int_0^t \varepsilon_t{}^2(t)dt. \end{cases} \tag{2}$$

The dissipated energy of the specimen is expressed as [27]

$$W_A(t) = W_i(t) - W_r(t) - W_t(t). \tag{3}$$

Under different environments, the energy dissipation rate of specimens directly reflects the strength of energy dissipation. The energy dissipation rate can be defined as the ratio of the dissipated energy of specimens to the incident energy [27].

$$\eta = \frac{W_A(t)}{W_i(t)}, \tag{4}$$

where $\varepsilon_i(t)$, $\varepsilon_r(t)$, and $\varepsilon_t(t)$ are the incident strain, reflected strain, and transmitted strain at time t, respectively, dimensionless; l_s is the thickness of specimen (m); C_0, E are the compressional wave velocity and elastic modulus of the compression bar (m/s and MPa), respectively; A, A_S are the cross-sectional area of the pressure bar and the cross-sectional area of the specimen (m^2); and W_i is incident energy, W_r is reflected energy, W_t is transmitted energy, and W_t is dissipated energy (J).

3. Test Results and Analysis

3.1. Stress-Strain Curves of Specimens. In order to control the variables and study the influence of low temperature on the dynamic mechanical properties of saturated concrete, 0.25 MPa air pressure was used to impact the specimen in the test. The stress-strain curve of low-temperature and saturated concrete is shown in Figure 4, and that of low-temperature and natural concrete is shown in Figure 5.

In order to better explain the characteristics of saturated water concrete under the coupling action of low temperature and dynamic load, the dynamic stress-strain curve of low-temperature concrete specimen (natural) in Figure 5 is

Figure 3: SHPB test device with variable cross section of 74 mm diameter.

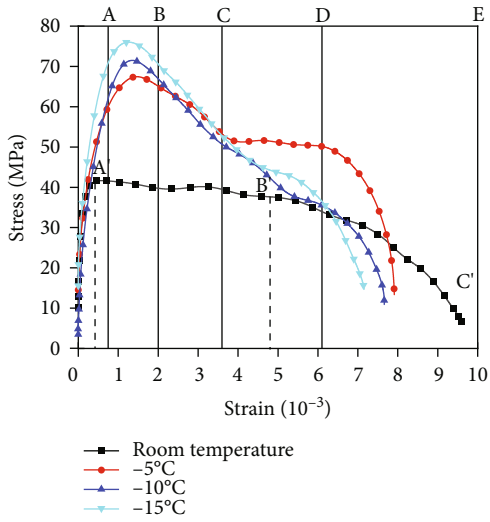

Figure 4: Dynamic stress-strain curve of frozen concrete elements (saturated).

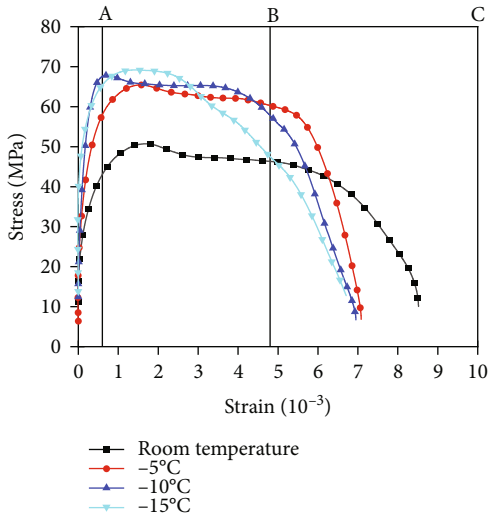

Figure 5: Dynamic stress-strain curve of frozen concrete elements (natural).

compared. It can be seen that under the condition of the same coupling value of low temperature and dynamic load, the dynamic stress-strain curve of saturated concrete changes obviously from that under natural state. The most significant difference can be seen from the stress peak value. At normal temperature, the dynamic strength peak value of saturated concrete is lower than that of natural state, while at low temperature, the strength peak value of saturated concrete is higher than that of natural state. It can also be seen from the stress-strain curve that concrete under different temperatures in the natural state has obvious dynamic yield platform stage, while concrete under normal temperature under saturated state and concrete under natural state both have obvious yield platform stage. However, at low temperature, the platform at the yield stage of saturated concrete is not obvious and becomes "steeper." In order to further reveal the characteristics of saturated concrete under the coupling action of low temperature and dynamic load, the dynamic stress-strain curve of low-temperature and saturated concrete in Figure 4 was analyzed in detail.

It can be seen from Figure 4 that the dynamic stress-strain curve of low-water-saturated concrete mainly includes three stages. (1) The OA stage in Figure 4 is stress-increasing stage, where the stress-strain curve is linear elastic stage. The crack in concrete gradually develops. When approaching to elastic limit, the strain increases fast. (2) In the second stage of stress decline, the stress plateau gradually decreases at normal temperature, while the stress rapidly decreases at low temperature and then decreases slowly at CD. The main reason is that with the penetration of microcracks, the internal integrity of the specimen structure is aggravated, the load transfer route is constantly reduced, and the bearing capacity decreases. At room temperature, the water particles in saturated concrete play a lubricating role in the bite force and friction between concrete and aggregate, so that the force is more uniform. For low-water-saturated concrete, the crack is filled with ice, which makes the strength of concrete increases. Hence, the strength of the concrete specimen with decreasing of temperature. Due to the increase of ice body, the original porous concrete medium is filled with brittle ice body, but after the late decline, there is a small area of slow decline. The analysis of the reason mainly considers that in the process of crack propagation, the occluded and frictional energy generated between aggregates will weaken the freezing effect of ice body and produce certain deformation under the action of stress. (3) In the DE section of specimen stress rapid decline stage, as the specimen cracks, the specimen is broken and the cohesion of the structure is almost exhausted.

3.2. Energy Time History Curve of Concrete Specimens with Low Water and Sufficient Water. Dynamic mechanical properties and energy calculation results of impact specimens are

Table 1: Test conditions and calculation results.

No.	Water content	Temperature (°C)	Height (mm)	Diameter (mm)	Dynamic compressive strength (MPa)	Strain rate (s^{-1})	Peak strain (10^{-3})	Incident energy (J)	Reflected energy (J)	Transmission energy (J)	Absorbed energy (J)	Energy dissipating rate-η (%)
5-1	Saturated	Room temperature	38.02	75.51	40.16	40.05	9.60	33.87	22.70	0.38	10.79	31.86
5-2			38.49	75.69	42.70	40.15	9.12	33.88	22.14	0.42	11.32	33.41
5-3			38.12	75.44	41.59	40.29	9.54	33.45	21.98	0.46	10.89	32.56
6-1		-5°C	38.28	75.77	67.44	38.57	7.91	33.19	15.86	0.93	16.4	49.41
6-2			38.56	75.46	68.50	38.41	8.01	33.46	15.79	0.95	16.72	49.97
6-3			38.99	75.66	65.20	38.65	7.95	33.52	16.01	0.99	16.52	49.28
7-1		-10°C	38.48	75.39	71.49	37.54	7.66	33.61	14.2	0.83	18.58	55.28
7-2			38.18	75.89	73.16	37.23	7.81	33.63	14.92	0.85	17.86	53.11
7-3			38.96	75.46	69.23	37.46	7.58	33.24	13.98	0.86	18.4	55.35
8-1		-15°C	38.28	75.61	76.02	36.99	7.15	33.38	12.79	0.85	19.74	59.14
8-2			38.56	75.69	75.42	37.05	7.49	33.94	12.06	0.82	21.06	62.05
8-3			38.46	75.44	78.12	36.95	7.12	33.78	12.86	0.81	20.11	59.53
1-1	Natural	Room temperature	38.48	75.67	50.69	39.96	8.51	33.04	18.65	0.51	13.88	42.01
1-2			38.20	75.78	49.15	39.04	8.01	33.44	19.04	0.49	13.91	41.60
1-3			38.94	75.98	51.20	39.55	7.89	33.64	18.05	0.47	15.12	44.95
2-1		-5°C	38.44	75.47	65.41	37.57	7.08	33.42	14.13	0.96	18.33	54.85
2-2			38.23	75.46	64.13	38.01	7.14	33.41	14.88	0.94	17.59	52.65
2-3			38.41	75.66	63.21	38.12	7.35	33.59	14.56	0.95	17.76	52.87
3-1		-10°C	38.82	75.28	67.85	37.05	6.94	33.80	13.40	0.96	19.44	57.51
3-2			38.16	75.14	69.12	36.85	6.82	33.45	13.12	0.92	18.64	55.72
3-3			38.51	75.29	65.33	36.97	7.01	33.94	13.89	0.91	19.14	56.39
4-1		-15°C	38.44	75.39	69.17	36.85	6.70	33.05	11.88	0.90	20.27	61.33
4-2			38.65	75.44	68.24	36.47	6.65	33.46	11.99	0.89	20.58	61.51
4-3			38.21	75.02	70.94	36.59	6.59	33.01	12.24	0.88	19.89	60.25

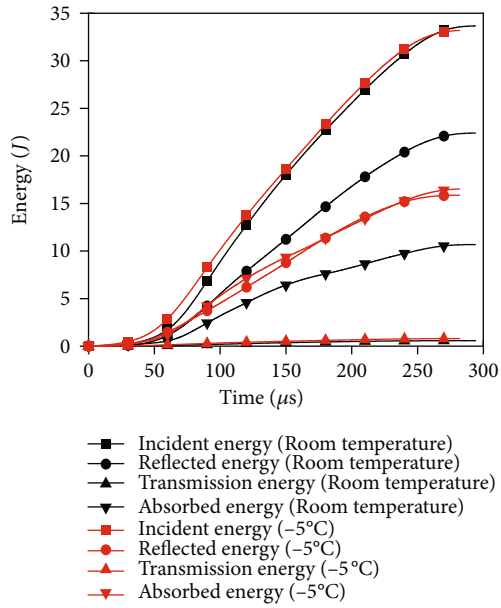

Figure 6: Energy distribution of saturated concrete.

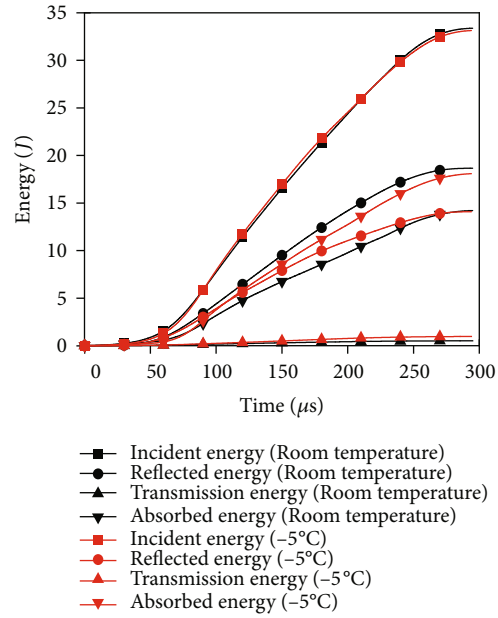

Figure 7: Energy distribution of natural concrete.

shown in Table 1 through data processing and theoretical calculation. Under the action of the same impingement air pressure, the relationship between incident energy, reflected energy, transmitted energy, and time of saturated concrete and natural concrete at room temperature and -5°C is shown in Figures 6 and 7.

It can be seen from Figures 6 and 7 that the initial kinetic energy obtained by bullets under the action of the same air pressure is the same, so the impact incident energy of the specimen is approximately the same, which also indicates the reliability of the test equipment. It can be seen from the figure that all kinds of energies increase with the increase of acting time, and the energy changes are not obvious between 0 and 50 μs. After 50 μs, the growth slope of absorbed and reflected energy is faster than that of transmitted energy. For saturated concrete at normal temperature, the reflected energy is higher than that at -5°C, and the transmitted energy is lower than that at -5°C, as shown in Figure 6 according to the conservation of energy. Satisfying the water absorption of low-temperature concrete is greater than the normal temperature condition, the natural conditions at room temperature, and low temperature state energy time history curve with a similar pattern, size is not the same, but the energy difference is also different. The difference between the reflected energy and absorbed energy of water-saturated concrete at room temperature is large, but the maximum absorbed energy of water-saturated concrete at -5°C is slightly larger than the reflected energy. However, for the same temperature, the value of reflected energy is greater than that of absorbed energy. The above results show that the saturated state has significant influence on the energy dissipation of concrete at both room temperature and low temperature.

3.3. Relationship between Temperature and Dynamic Compressive Strength and Peak Strain of Water-Saturated Specimens. From the analysis of Section 2.2 and Table 1, it can be seen that the water-saturated state has a greater impact on the strength of concrete, and it can be seen from the table that the ratio of the strength of the water-saturated concrete to the strength of the natural state is 0.82, indicating that the water-saturated water molecules have a deteriorating effect on the dynamic strength of the concrete, and when the temperature reaches -15°C, the strength ratio of the water-saturated concrete to the strength in the natural state is 1.10, indicating that the transformation of water molecules into ice molecules has a certain enhancement effect on the dynamic strength of the concrete. There is a certain low temperature state that can compensate for the deterioration effect of saturation. In order to further reveal the relationship between the dynamic strength of water-saturated concrete under low temperature and dynamic load and the relationship between peak strain and low temperature of water-saturated concrete under low temperature and dynamic load, the law of concrete under water-saturated state is more detailed, and the relationship between low-temperature dynamic compressive strength and peak strain of natural concrete is compared and analyzed, and the relationship between dynamic compressive strength and peak strain and temperature of water-saturated concrete is obtained as shown in Figures 8 and 9.

It can be seen from Figure 8 that under test conditions, the dynamic strength of saturated concrete increases linearly with the decrease of temperature. After linear fitting of data, the linear correlation coefficient between dynamic strength of saturated concrete and temperature is $R^2 = 0.998$. The dynamic compressive strength of saturated concrete increases by 34.37 MPa when it drops from normal temperature to -15°C. Compared with the natural state, state full water dynamic compressive strength of concrete under normal temperature is low, the analysis reason mainly is a kind

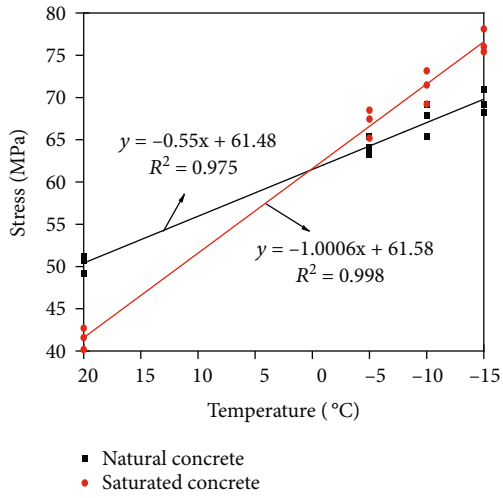

Figure 8: Relationship between dynamic strength and temperature of saturated concrete.

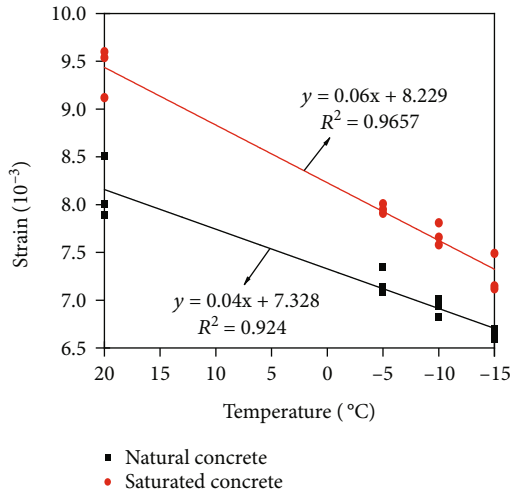

Figure 9: Relationship between peak strain and temperature of saturated concrete.

of porous concrete is hydrophilic material, feed water condition of concrete softening of water particles and lubrication, and creep tendency, so that normal temperature state full of water dynamic compressive strength of concrete material has weakened a lot. As the temperature decreases, it can be seen from the fitting curve that the dynamic compressive strength of concrete under saturated water is equivalent to that under natural state between 0°C~-2°C. However, the effect of temperature is not considered in the test, but the results are reliable combined with theoretical analysis. When the temperature is lower than 0°C, the free water in concrete turns into ice crystal. On the one hand, the crystal has a certain strength to fill the void of concrete; on the other hand, the process of freezing water into ice under the effect of low temperature increases the cohesion and internal friction angle of the specimen itself, which weakens the softening and lubrication effect of water together. Within the test range, when the temperature reaches lower temperature, the dynamic strength of saturated concrete increases, and the main reason can be explained by the model of friction crack slip [28–35]. Concrete is subject to impact load, cracks will develop and extend from the microcracks in the specimen, and for this moment, the concrete can still withstand a large load; cracks in the development and extension of the original cracks will produce friction slip between the cracks that have been generated. Concrete friction slip needs to overcome the following aspects of resistance: (1) the adhesion force between the two friction surfaces and (2) the resistance encountered when the concave and convex particles cross each other, which is closely related to the roughness of the friction surface, and for the destruction of low-temperature water-saturated concrete, the ice crystal structure will increase the adhesion of the friction face and will also increase the roughness of the friction surface. In the crack propagation, the friction resistance of ice crystal structure slip is the most important factor. The lower the temperature is, the greater the friction resistance of slip is, and the higher the stress of crack initiation and growth is, and the compressive strength also increases. The schematic diagram of the slip model is shown in Figure 10.

Considering the linear increase of concrete with temperature decrease in natural state, the correlation coefficient of fitting is $R^2 = 0.991$. At -15°C, the peak value dynamic compressive strength of concrete increases by 18.48 MPa. It can be seen that the effect of peak compressive strength of saturated concrete changing with temperature is significantly higher than that of dry concrete. According to Figure 10, the concrete material itself has many holes in the natural state. Under the impact load, the crack propagation in the concrete preferentially passes through the weak surface and holes of the specimen, and the crack penetrates the weak surface and holes along the stress direction. For saturated concrete, due to lubrication and softening, the energy consumed by cracks running through concrete is weakened. For the same crack, the energy required is smaller, and the overall bearing capacity of saturated concrete specimens is reduced. However, at low temperature, the water in the holes and voids of saturated concrete is filled with ice crystals, and the filling strength of ice crystals is higher, which makes the failure mode of concrete more inclined to axial splitting and tensile failure. The crack produced by the specimen is more parallel to the stress path, which reduces the guiding effect of the weak face on the crack propagation, thus improving the strength of the specimen as a whole.

Based on the relationship between peak strain and temperature of saturated concrete in Figure 9, it can be seen that the peak strain of saturated concrete decreases linearly with the increase of temperature, and the linear correlation coefficient is $R^2 = 0.97$. For concrete under natural condition, the peak strain of saturated concrete is always greater than that of concrete under natural condition when it drops from normal temperature to -15°C in the test range. However, the change rate of peak strain with temperature of saturated concrete (slope 0.06) is larger than that of natural concrete (slope 0.04). It can be seen that with the continuous decrease

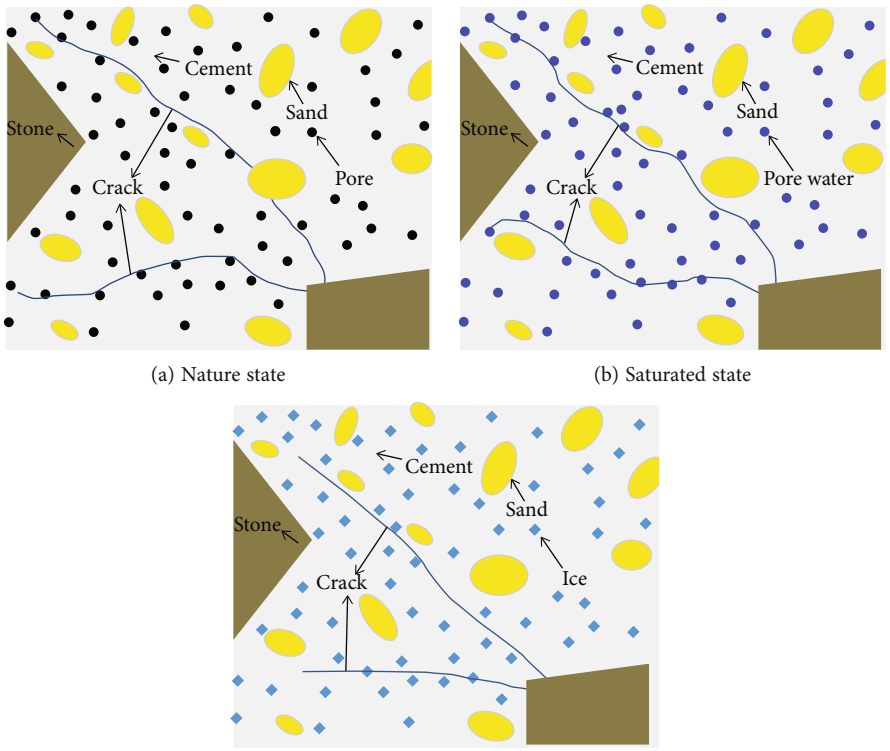

(a) Nature state

(b) Saturated state

(c) Low temperature condition state

Figure 10: Schematic diagram of failure model of water-saturated concrete.

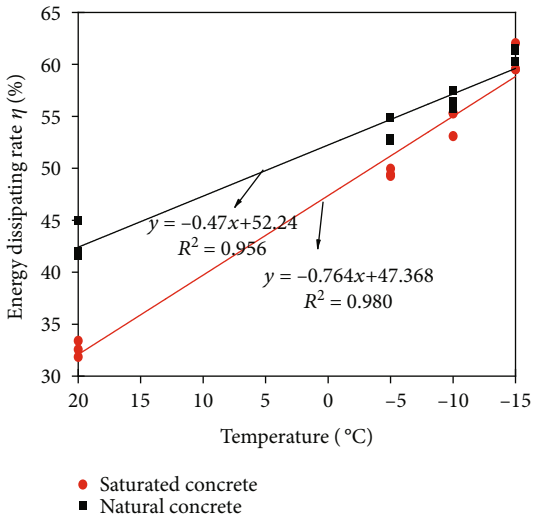

Figure 11: Relationship between energy dissipation rate of water-saturated concrete and temperature.

of temperature, the peak strain of saturated concrete will be smaller than that of concrete under natural state. The main reasons are as follows: first, with the decrease of temperature, the brittleness of ice crystal structure in saturated concrete becomes stronger. At the same time, considering the frost heave effect of ice crystal structure, the strength of saturated concrete increases within the test temperature range, and free water is mainly frozen inside the structure, which mainly produces filling and solidification. Second, with the decrease of temperature, the bound water inside the structure, including aggregate and sand, will also freeze, which will cause frost heave damage to the structure. Therefore, with the continuous decrease of temperature, the dynamic limit strain of saturated concrete will gradually decrease [36].

3.4. The Relationship between Energy Dissipation Rate and Temperature. Under different environments, the energy dissipation rate of specimens directly reflects the strength of energy dissipation. Based on Table 1, the relationship between the energy dissipation rate of saturated concrete and temperature is shown in Figure 11.

Figure 11 shows that the energy dissipation rate of saturated concrete increases linearly with the decrease of temperature, and the linear correlation coefficient $R^2 = 0.98$. Combined with Figure 6, the failure energy absorption process of saturated concrete specimens was analyzed from the perspective of absorbed energy and energy dissipation. In the initial stage of impact, the stress wave was in the rising edge, and the saturated concrete specimens were in the stage of elastic deformation. The absorbed energy of saturated concrete was stored in the form of elastic energy. With the increase of incident energy, due to the wave impedance mismatch between the specimen and the pressure bar, the incident end face of the specimen generates reflection energy, and the poststress wave propagates back and forth through the specimen in the transmission bar, specimen, and incident bar, and each energy is supplemented. As the stress wave strength is greater than the ultimate compressive

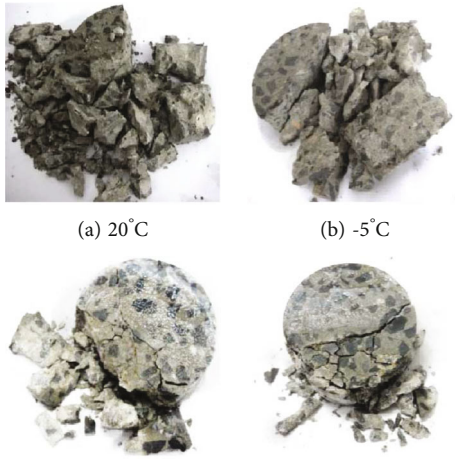

(a) 20°C (b) -5°C

(c) -10°C (d) -15°C

Figure 12: Failure pattern of water-filled concrete.

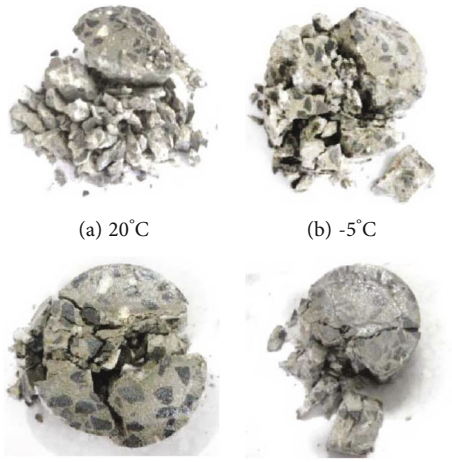

(a) 20°C (b) -5°C

(c) -10°C (d) -15°C

Figure 13: Failure pattern of natural concrete.

strength of saturated concrete, damage evolution and accumulation will occur in the saturated concrete specimen. The primary microcracks in saturated concrete expand and produce a large number of new microcracks at the same time, and the absorption energy continues to increase, which is also the main stage of energy dissipation. With lower temperature, the microcracks of concrete internal full water, microdefects by ice crystals, and low temperature damage will not be able to make full water concrete according to the original crack, weak surface development, and thus need to consume more energy, but with the lower temperature, feed water concrete and concrete energy dissipation is gradually close to nature.

The main reason is that with the decrease of temperature, regardless of saturated concrete and concrete in natural state, the bound water inside the structure, including aggregate, sand, and other internal water, also freezes, and the overall brittleness of the specimen becomes stronger. The dynamic compressive strength of concrete with low water and sufficient water will increase, but it is more likely to be broken, and the overall energy dissipation rate will tend to be the same when the ultimate strain decreases.

3.5. Fracture Morphology Characteristics. Figures 12 and 13 show the failure patterns of concrete in low water and full water and concrete in natural state at different temperatures.

It can be seen from Figure 12 that, under the impact of the same air pressure, the fragmentation of saturated concrete gradually increases with the decrease of temperature, and the integrity of specimens gradually improves. The decrease of temperature can improve the impact resistance of saturated concrete, which is consistent with the failure law of natural state concrete. The axial splitting tensile failure and compression shear failure of concrete specimens with low temperature and adequate water are the main. As the temperature decreases, the crushing state changes from crushing to axial splitting failure, and the axial through-crack gradually decreases. Saturated concrete is seriously

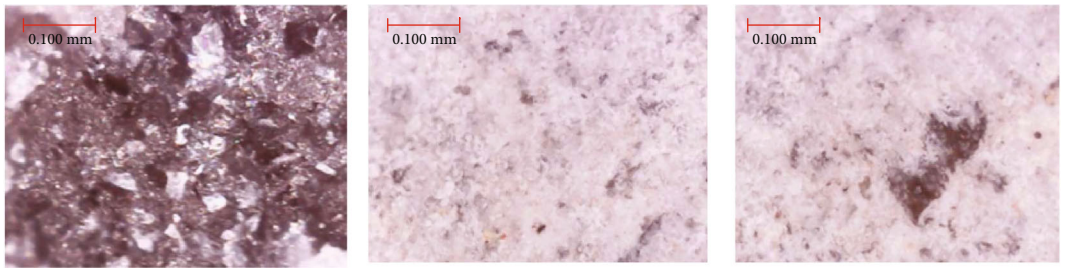

(A) Aggregate meso structure (B) Cement meso structure (C) Cement and mortar meso structure

(a) Mesostructure of concrete surface in natural state

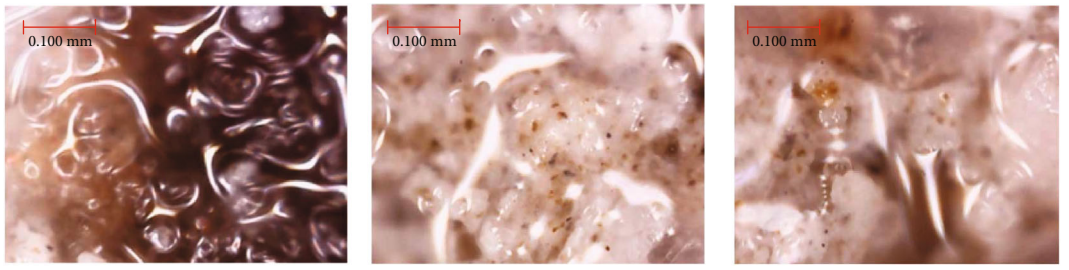

(A) Aggregate meso structure (B) Cement meso structure (C) Cement and mortar meso structure

(b) Mesostructure of concrete surface under saturated state

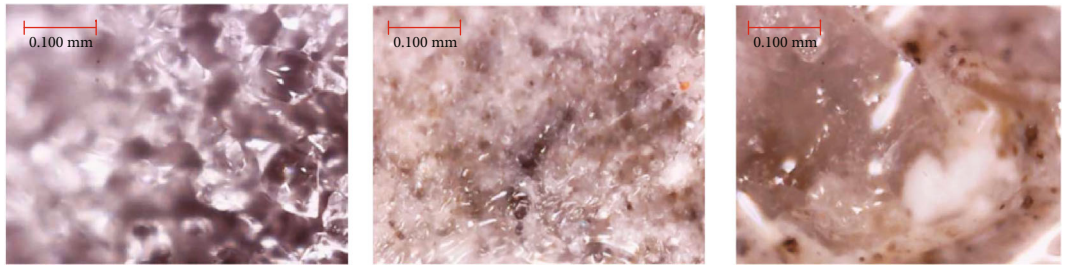

(A) Aggregate meso structure (B) Cement meso structure (C) Cement and mortar meso structure

(c) Microstructure of frozen concrete surface under saturated condition

Figure 14: Failure pattern of concrete.

broken at room temperature, and the destruction range at low temperature is smaller than that at natural state. Based on the mesostructure of concrete, the damage and evolution of saturated concrete are studied by analyzing the physical and mechanical process of the change of mesostructure, which can well reveal the damage mechanism and law of saturated concrete. In order to reveal the mesostructure of fracture and fracture of low water-saturated concrete, the surface of water-saturated concrete specimen was observed by a bester electronic digital microscope with magnification of 1000 times. The observations are shown in Figure 14.

It can be seen from Figure 14 that there are a large number of voids and defects (such as cavities, holes, and microcracks) in concrete in the natural state. In the saturated state, voids and microcracks are filled by water, as shown in Figure 14(b). In the water-saturated low temperature state, the surface of concrete is filled with ice crystal particles, but the ice crystal particles do not completely fill and fill the pores and voids as expected. That is mainly because the process of freezing water does not just freeze at zero degrees Celsius. To turn water molecules into ice crystals, they need an attachment called a nucleus. For saturated concrete, water molecules will preferentially form lattice on the contact surface with concrete, sand, and cement and form ice body structure on this basis. Therefore, the ice body of saturated mortar does not always fill the pores. However, due to the action of ice crystals, the weak surface of concrete is effectively connected. Therefore, under the impact load, the dynamic process of concrete defects in the natural state is intensified, and microdefects in different parts of the interior are simultaneously activated and developed, resulting in a small number of cracks. Under the continuous action of stress waves, a large number of microdamage and microcrack development, coupled with the development of internal structural defects, will produce cracks in the internal structure of particles, along the cracks between particles and grain boundaries. However, the microstructure of concrete subjected to impact dynamic load is not easily changed by ice crystal structure, and the distribution of concrete will change from a free state to directional distribution under stress direction. When the specimen is subjected to uniaxial impact compression, after the stress wave reaches the

contact surface between the incident bar and the specimen, the effective stress in all parts of the specimen is uniform with the propagation of the stress wave in the concrete with low temperature and adequate water. With the further increase of the axial stress, the microdefects of the specimen develop along the axial stress direction and produce cracks. The cracks occur along the direction parallel to the compressive stress direction, through the two ends of the specimen, and produce axial splitting tensile failure.

4. Conclusions

In bridge foundation, water supply, and drainage project, immersed concrete faces frost heaving dangers under low-temperature state. Additionally, the concrete also faces dynamic failure, when many cars drive on it. Hence, the mechanics characteristics of water-saturated concrete under the coupling of low temperature and dynamic load are studied. Water saturation and dry concrete impact compression tests were conducted at a normal temperature of -5°C, -10°C, and -15°C using Φ74 mm split Hopkinson pressure rod (SHPB). The following conclusions are reached:

(1) In the case of the same coupling value of low temperature and dynamic load, under normal temperature, the strength ratio of water-saturated concrete to natural state is 0.82, and the water molecules in the water-saturated state have a deteriorating effect on the dynamic strength of concrete, and when the temperature reaches -15°C, the strength ratio of water-saturated concrete to the strength in natural state is 1.10, and the transformation of water molecules into ice crystal structures has a certain enhancement effect on the dynamic strength of concrete. Under different temperatures, concrete in the natural state and the natural state of normal temperature and water-saturated concrete have obvious dynamic yield platform stage, but at low temperature, the yield stage of water-saturated concrete platform is not obvious, and the material properties become more and more "steep" and brittle

(2) In the range of the test, the various energies increase with the time of action. There is no obvious change of each energy between 0 and 50 μs. After 50 μs, the increase slope of absorbed and reflected energy is faster than that of transmitted energy. For saturated concrete at room temperature, the reflection energy is higher than -5°C, and the transmission energy is lower than -5°C. The energy dissipation rate of saturated concrete increases linearly with the decrease of temperature

(3) Under the experimental conditions, the dynamic strength of saturated concrete increases linearly with the decrease of temperature, and the dynamic compressive strength of saturated concrete increases by 34.37 MPa when the temperature drops from 20°C to -15°C at normal temperature. The peak strain of saturated concrete decreases linearly with the increase of temperature. For concrete under natural condition, the peak strain of saturated concrete is always greater than that of concrete under natural condition when it drops from normal temperature to -15°C within the test range. However, the change rate of peak strain with temperature of saturated concrete (slope 0.06) is larger than that of natural concrete (slope 0.04).

(4) The results of the thesis study have certain theoretical reference value for the design, construction, maintenance and reinforcement of bridge foundation concrete, water supply, and drainage engineering building structures and outdoor low-temperature concrete pavement in cold areas, and for concrete structures that need to be built in water and withstand dynamic load, it should be selected to increase silicon powder and other fine admixtures to reduce bubbles in concrete, or to select concrete with higher strength labels to reduce the effect of saturation deterioration. For the water-saturated concrete structure in the cold area, although under the action of low temperature dynamic load, the strength of the concrete increases, but the brittleness of the concrete increases, especially for some important structures, the sudden instability of the brittle damage is unpredictable, which will bring very serious disasters, for these places should improve the reinforcement rate of the concrete structure or increase the steel fiber; carbon fiber, polyester fiber, etc. can improve the overall ductility of the concrete under the condition of ensuring the strength of the concrete

Data Availability

All data included in this study are available upon request by contact with the corresponding author.

Conflicts of Interest

The authors declare no conflict of interest.

Acknowledgments

This work was supported by Anhui Province Key Laboratory of Building Structure and Underground Engineering, Anhui Jianzhu University, Hefei (KLBSUE-2022-03), and the High-Level Talent Introduction Scientific Research Start-Up Fund of Anhui University of Science and Technology.

References

[1] Y. J. Xie, W. Liu, B. J. Liu, and X. Feng, "Experimental study of com-pressive strength of early-strength con crete cured under low temperatures for Qinghai-Tibet railway," *Bridge Construction*, vol. 2, p. 27, 2003.

[2] L. P. Gu, "Quality control of low(minus)-temperature, early-strength and high-performance concrete of Qinghai-Tibet railway project in frozen plateau area," *Journal of Railway Engineering Society*, vol. 1, pp. 34–38, 2004.

[3] T. J. MacLean and A. Lloyd, "Compressive stress–strain response of concrete exposed to low temperatures," *Journal of Cold Regions Engineering*, vol. 33, no. 4, 2019.

[4] J. Xie, X. M. Li, and H. H. Wu, "Experimental study on the axial-compression performance of concrete at cryogenic temperatures," *Construction and Building Materials*, vol. 72, pp. 380–388, 2014.

[5] S. L. Gao and P. X. Xie, "Effect of temperatures and moisture content on the fracture properties of engineered cementitious composites (ECC)," *Materials*, vol. 15, no. 7, pp. 2604–2604, 2022.

[6] J. J. Guo, Z. Zhang, J. J. Wu et al., "Early-age mechanical characteristics and microstructure of concrete containing mineral admixtures under the environment of low humidity and large temperature variation," *Materials (Basel)*, vol. 14, no. 17, p. 5085, 2021.

[7] C. Y. Xu, Y. Qin, M. Li, and H. M. Liu, "Service performance analysis and stability evaluation of concrete face slab of Nazixia Dam," *Engineering Journal of Wuhan University*, vol. 53, no. 7, pp. 565–573, 2020.

[8] C. X. Wang, J. Xie, and H. J. Li, "Experimental research on the properties of concrete under low-temperature," *Engineering Mechanics*, vol. 28, no. S2, pp. 182–186, 2011.

[9] N. Zhang, J. Liao, W. Z. Ji, B. H. Wang, D. H. Zhang, and Y. W. Li, "Low temperature mechanical properties and test methods of concrete," *Journal of the Chinese Ceramic Society*, vol. 42, no. 11, pp. 1404–1408, 2014.

[10] L. Dahmani, A. Khenane, and S. Kaci, "Behavior of the reinforced concrete at cryogenic temperatures," *Cryogenics*, vol. 47, no. 9, pp. 517–525, 2007.

[11] Y. T. Wang, J. Y. Pang, and X. Huang, "Experimental research on compressive strength of rubber concrete with different particle sizes at low temperature," *Bulletin of the Chinese Ceramic Society*, vol. 38, no. 7, pp. 2308–2313, 2019.

[12] Q. Wang, Y. Y. Wang, and H. F. Xing, "An experiment research of mechanics performance of polypropylene fiber concrete under freezing temperature," *Journal of Shihezi University(Natural Science)*, vol. 2, pp. 229–231, 2007.

[13] Y. U. Liang-shu, X. U. Qing-yu, W. A. N. G. Wen-jin, and W. Li-yan, "Study on behaviors of asphalt concrete under low temperature," *Journal of Hydraulic Engineering*, vol. 5, pp. 634–639, 2006.

[14] Z. Fang, S. K. Liu, Z. Y. Huang, and J. T. Chen, "Flexural properties of ultra-high performance concrete under different temperatures," *Journal of the Chinese Ceramic Society*, vol. 48, no. 11, pp. 1732–1739, 2020.

[15] S. Chen, S. Q. Shi, Q. L. He, and J. Li, "Experimental study and numerical simulation on the impact resistance performance of concrete reinforced with metal meshes," *Materials Reports*, vol. 34, no. 20, pp. 20046–20052, 2020.

[16] W. H. Zhang, P. Y. Liu, and Y. J. Lyu, "Dynamic mechanical property of UHPCs: a review," *Materials Reports*, vol. 33, no. 19, pp. 3257–3271, 2019.

[17] S. L. Fan, S. Y. Zhao, B. X. Qi, and Q. Kong, "Damage evaluation of concrete column under impact load using a piezoelectric-based EMI technique," *Sensors*, vol. 18, no. 5, p. 1591, 2018.

[18] Y. He, M. Gao, H. Zhao, and Y. Zhao, "Behaviour of foam concrete under impact loading based on SHPB experiments," *Shock and Vibration*, vol. 2019, Article ID 2065845, 13 pages, 2019.

[19] H. Zhu, A. Liu, and Y. Yu, "Low temperature impact performance of basalt fiber reinforced concrete," *Journal of Materials Science and Engineering*, vol. 36, no. 4, pp. 600–604, 2018.

[20] B. F. Huang and Y. Xiao, "Impact tests of high-strength, lightweight concrete with large spilt Hopkinson pressure bar," *China Civil Engineering Journal*, vol. 54, no. 2, pp. 30–42, 2021.

[21] R. Y. Huang, L. L. Hu, J. Qin, D. Jiang, and L. Meng, "Effect of free water on the mechanical properties and blast resistance of concrete," *KSCE Journal of Civil Engineering*, vol. 25, no. 8, pp. 3084–3096, 2021.

[22] J. Liu, X. L. Du, and G. W. Ma, "Macroscopic effective moduli and tensile strength of saturated concrete," *Cement and Concrete Research*, vol. 42, no. 12, pp. 1590–1600, 2012.

[23] Q. F. Wang, Y. H. Liu, and G. Peng, "Effect of water pressure on mechanical behavior of concrete under dynamic compression state," *Construction and Building Materials*, vol. 125, pp. 501–509, 2016.

[24] D. M. Yan, K. H. Liu, H. D. Li, and S. L. Xu, "A study on the dynamic compressive behavior of pre-damaged concrete," *Journal of Hydraulic Engineering*, vol. 46, no. 9, pp. 1110–1118, 2015.

[25] B. Sun, H. Liu, D. Yuan, F. L. Wang, and S. Zeng, "Damage characteristics of uni-body bi-material specimen for rock-concrete under dry and saturated states," *Bulletin of the Chinese Ceramic Society*, vol. 38, no. 2, pp. 482–487, 2019.

[26] Y. X. Wang, J. Y. Xu, and Y. G. Yin, "Basic properties of water saturated geopolymeric concrete," *Bulletin of the Chinese Ceramic Society*, vol. 35, no. 12, pp. 4237–4241, 2016.

[27] L. Song and S. S. Hu, "Two-wave and three-wave method in SHPB data processing," *Explosion and Shock Waves*, vol. 25, no. 4, pp. 368–373, 2005.

[28] S. J. Liu, L. X. Wu, J. Z. Wang, Y. H. Wu, and Y. Q. Li, "Remote sensing-rock mechanics(VI)-features of rock friction-sliding and analysis on its influence factors," *Chinese Journal of Rock Mechanics and Engineering*, vol. 8, pp. 1247–1251, 2004.

[29] Z. Tao, Q. Geng, C. Zhu et al., "The mechanical mechanisms of large-scale toppling failure for counter-inclined rock slopes," *Journal of Geophysics and Engineering*, vol. 16, no. 3, pp. 541–558, 2019.

[30] Q. Wang, S. Xu, Z. Xin, M. He, H. Wei, and B. Jiang, "Mechanical properties and field application of constant resistance energy- absorbing anchor cable," *Tunnelling and Underground Space Technology*, vol. 125, article 104526, 2022.

[31] Q. Wang, S. Xu, M. He, B. Jiang, H. Wei, and Y. Wang, "Dynamic mechanical characteristics and application of constant resistance energy-absorbing supporting material," *International Journal of Mining Science and Technology*, vol. 32, no. 3, pp. 447–458, 2022.

[32] M. Z. Gao, B. G. Yang, J. Xie et al., "The mechanism of microwave rock breaking and its potential application to rock-breaking technology in drilling," *Petroleum Science*, vol. 19, no. 3, pp. 1110–1124, 2022.

[33] P. Zhang, D. Zhang, Y. Yang et al., "A case study on integrated modeling of spatial information of a complex geological body," *Lithosphere*, vol. 2022, no. Special 10, article 2918401, 2022.

[34] Z. Dou, S. Tang, X. Zhang et al., "Influence of shear displacement on fluid flow and solute transport in a 3D rough fracture," *Lithosphere*, vol. 2021, no. Special 4, article 1569736, 2021.

[35] Q. Yin, J. Wu, Z. Jiang et al., "Investigating the effect of water quenching cycles on mechanical behaviors for granites after conventional triaxial compression," *Geomechanics and Geophysics for Geo-Energy and Geo-Resources*, vol. 8, no. 2, p. 77, 2022.

[36] Y. Wang, Y. L. Li, and C. X. Liu, "Dynamic mechanical behaviors of ice at high strain rates," *Explosion and Shock Waves*, vol. 31, no. 2, pp. 215–219, 2011.